SDC

OPEN

CORRELATION BETWEEN POSTERIOR STAPHYLOMA AND DOME-SHAPED MACULA IN HIGH MYOPIC EYES

FANGFANG DAI, MD,* SHUYIN LI, BS,* YANTING WANG, MS,* SHUANGSHUANG LI, BS,† JINFENG HAN, BS,† MENGDI LI, BS,† ZHONG ZHANG, BS,‡ XUEMIN JIN, MD,* SHEWEI DOU, BS‡

Purpose: To investigate the relationship between posterior staphyloma and dome-shaped macula (DSM) in highly myopic eyes.

Methods: The clinical data were collected from patients with high myopia: diopter, best-corrected visual acuity, axial length, fundus images, optical coherence tomography, and 3D magnetic resonance imaging. A DSM was defined as a convex curvature of the macula in one or both of the vertical and horizontal optical coherence tomography scans. The relationship between DSM and posterior staphyloma was evaluated.

Results: A total of 123 eyes were included. Dome-shaped macula was found in 18 eyes (14.63%). Twelve eyes with DSM had positive 3D magnetic resonance imaging findings. Nine eyes had horizontal oval-shaped dome, and a band-shaped inward convexity that extended horizontally from the optic disc through the fovea could be seen. Three eyes had round dome, and 3D magnetic resonance imaging showed a round inward convexity of the macular area. Five inward convexities were the border of multiple staphylomas, five were the boundary of one staphyloma, and two were within a single staphyloma.

Conclusion: The formation of highly myopic DSM is related to the morphological change of the entire posterior segment.

RETINA 40:2119–2126, 2020

Dome-shaped macula (DSM) was firstly proposed by Gaucher et al[1] in 2008 and was defined as an inward protrusion of macula, which occurs in a dome-shaped formation as visualized by optical coherence tomography (OCT). Since then, many theories have been developed regarding the cause of the disease. The possibility of "low intraocular pressure" and "vitremacular traction syndrome" was excluded because no objective element supported these hypotheses.[2] Consequently, Soudier et al[3] followed up 29 DSM patients for 6 to 111 months identifying increased macular bulge height. In another study, they detected decreased choroidal thickness at the periphery but not in the macular area with DSM.[4] Thus, they proposed that DSM might be caused by scleral introversion in resisting the development of staphyloma.[4] Furthermore, Byeon et al suggested that DSM might be associated with posterior staphyloma (PS) (condition which includes extensive protruding of posterior pole plus macular protrusion, extensive protruding of posterior pole plus peripapillary protrusion, and extensive protruding of posterior pole plus inferior staphyloma) or heteromorphosis of the inferior staphyloma. Assuming that the sclera is the thinnest at its peak protrusion area, the macular scleral thickening symptom occurring with complicated staphyloma is a reasonable

From the *Department of Ophthalmology, Henan Provincial People's Hospital, People's Hospital of Zhengzhou University, Henan Eye Institute, Henan Eye Hospital, Zhengzhou, China; †Zhengzhou University, Zhengzhou, China; and ‡Department of Radiology, Henan Provincial People's Hospital, People's Hospital of Zhengzhou University, Zhengzhou, China.

Supported by two projects of Science and Technology Department of Henan Province (CN), "High Myopia 3D Imaging and Macular Surgery" (project number: 162102410004) and "Image and Artificial Intelligence Research and Development Platform of Henan Eye Hospital."

None of the authors has any conflicting interests to disclose.

Supplemental digital content is available for this article. Direct URL citations appear in the printed text and are provided in the HTML and PDF versions of this article on the journal's Web site (www.retinajournal.com).

Reprint requests: Xuemin Jin, MD, Henan Provincial People's Hospital, People's Hospital of Zhengzhou University, Henan Eye Institute, Henan Eye Hospital, Zhengzhou,45000 China; e-mail: 2740913223@qq.com

hypothesis.[5] Recently, Ellabban et al[6] have performed a study on 35 eyes with DSM and high myopic patients revealing that sclera thinning at the parafoveal area was more significant compared with the foveal center and that the macular areas in DSM patients underwent sclera thinning in a progressive and asymmetric manner.

The aforementioned studies have been mostly based on OCT investigation and interpretation, and limited scanning area has hindered the application of OCT in studying the relationship between DSM and PS. In recent years, three-dimensional (3D) magnetic resonance imaging (MRI), which has the ability to vividly display the morphology and scope of PS, as well as to reveal its relationship with the optic nerve, has been applied in examination of the PS in high myopic eyes.[7] This study utilized the same technique in combination with OCT to investigate the relationship between DSM and PS.

Materials and Methods

Subject Inclusion

This study included a total of 123 eyes in 69 high myopic patients who underwent 3D MRI eye examination at the Department of Ophthalmology in Henan Provincial People's Hospital from October 2016 to August 2017. Eyes were excluded if they had a preexisting obvious ocular disease or if they had a history of ocular surgery, other than cataract surgery and photorefractive keratectomy. The original refractive errors were used for eyes that underwent cataract surgery or photorefractive keratectomy. Following the informed consent, basic information and clinical results were collected from patients with high myopia (diopter $>$ 6.00 D). The clinical examination results included diopter, best-corrected visual acuity (LogMAR), axial length (Carl Zeiss IOLMaster(R) Advanced Technology V.5.4; Carl Zeiss Meditec, Inc, Oberkochen, Germany), fundus imaging, OCT (Carl Zeiss Meditec, Inc SW Ver: 4.5.1.11, or Optovue, Inc SW Ver: 2016.1.0.26; Fremont, CA, or Heidelberg Engineering, Inc SW Ver: 6.3.4; Heidelberg, Germany), and 3D MRI of eyeballs (Siemens Prism 3.0T or GE Discovery 750 plus 3.0T).

Fundus Imaging

Fundus images were obtained with a 45° fundus camera (VISUCAM 224; Zeiss) and wide-field fundus camera (Optomap plus; Optos PLC, Scotland, United Kingdom) to record fundus complications. High-myopia macular lesions were divided into the following: tessellated fundus, diffuse chorioretinal atrophy, patchy chorioretinal atrophy, and macular hemorrhage (myopic choroidal neovascularization and simple macular hemorrhage).[8]

Optical Coherence Tomography

Optical coherence tomography scan modes included oblique scanning through the macular fovea to optic disc and horizontal and vertical multiline scanning in macular area. Referring to the definition of DSM reported by previous studies,[6,9] the diagnosis of DSM configuration was based on the presence of an inward bulge of the retinal pigment epithelium line. And the macula bulge height, the distance between the retinal pigment epithelium at the foveal center and the connection line of the bilateral lowest points of the retinal pigment epithelium curvature, was greater than 50 μm on the most convex vertical or horizontal OCT sections. More specifically, DSM detected by horizontal scan was named "vertical oval-shaped dome"; those detected by vertical scan were called "horizontal oval-shaped dome," and those detected by both methods were named "round dome."[9]

3D Magnetic Resonance Imaging

The method for 3D MRI scanning has been described in our previous studies.[10] Briefly, a magnetic resonance scanner and 32-channel head coil were used while the patient was in a supine position. After closing the eyelid, the 3D sequence MRI scanning of the eye was applied. Sagittal cube imaging technique T2WI-fs was used with the time of repetition of 2000.0 ms and time of echo 110.0 $\sim$ 120.0 ms. One twenty-eight layers with layer thickness of 0.6 $\sim$ 0.8 mm were collected with the scope of 256 mm $\times$ 230 mm. The scanning lasted 3 minutes 18 seconds, and the scanning range covered the whole head. Patients were advised to focus during scanning and to try not to move their heads or eyeballs. Data were transferred to ADW4.6 postprocessing workstation for volume rendering image reconstruction.

Based on the 3D eye MRI image, PS was defined as the symptom of partially convex posterior curvature of the eyeball with radius less than the curvature of the surrounding sphere.[11]

Statistical Analysis

The chi-square test was used to analyze categorical variables, which were described using frequencies and percentages. Continuous variables were compared and described using the *t*-test and means and standard deviations, respectively. We used SPSS statistics 20.0 software (IBM Corp) for all analyses. The associations

were considered to be statistically significant when $P < 0.05$.

Results

General Information and Basic Characteristics

A total of 123 eyes in 69 patients (19 males and 50 females) were included in this study. The average age was 49.70 ± 16.29 years old. Best-corrected visual acuity was 0.69 ± 0.47 LogMAR (Snellen visual acuity ratio 20/60) (except for one eye which was tested by hand motion and seven eyes by counting finger). The mean diopter was −16.7 ± 5.0 D, and the average axial length was 29.74 ± 2.04 mm. Patients had macular retinoschisis (56 eyes, 45.53%), paravascular retinal holes and retinoschisis (21 eyes, 17.07%), macular pucker (35 eyes, 28.46%), DSM (18 eyes, 14.63%), inner lamellar hole (14 eyes, 11.38%), and retinal detachment (15 eyes, 12.20%) (10 eyes of the 15 eyes had circumscribed macular retinal detachment, that is, subretinal fluid height was less than 200 μm. The range of retinal detachment in the other five eyes was confined to the posterior pole.), macular hole (6 eyes, 4.88%), peripapillary intrachoroidal cavitation (5 eyes, 4.07%), macular intrachoroidal cavitation (1 eye, 0.81%), outer lamellar hole (3 eyes, 2.44%), subretinal hemorrhage (2 eyes, 1.62%), patchy chorioretinal atrophy (24 eyes, 19.51%), and choroidal neovascularization-related macular atrophy (15 eyes, 12.20%).

A total of 18 eyes (14.63%) in 14 people had DSM in this study (Table 1). The mean age was 54.93 ± 13.34 years. There was no significant difference between the ages of people with DSM and without DSM (48.68 ± 16.52 years) ($P > 0.05$). The mean axial length of the eyes with DSM was 30.33 ± 1.88 mm, which was also not significantly different from that without DSM (29.64 ± 2.06 mm) ($P > 0.05$). According to the morphology of DSM on OCT, it was further divided into horizontal oval-shaped dome (14 eyes, 77.78%) and round dome (4 eyes, 22.22%). Among the eyes with a DSM, macular retinoschisis was seen in five eyes (27.78%), paravascular retinal holes and retinoschisis in two eyes (11.11%), macular pucker in three eyes (16.67%), peripapillary intrachoroidal cavitation in one eye (5.55%), patchy chorioretinal atrophy (12 eyes, 66.67%), choroidal neovascularization-related macular atrophy four eyes (22.22%), and no macular intrachoroidal cavitation, outer lamellar hole, and inner lamellar hole or subretinal hemorrhage. Two eyes (11.11%) with a macular hole were observed, and one of them was also combined with a shallow perihole retinal detachment.

Take the eyes without DSM as controls, neither the rate of choroidal neovascularization-related macular atrophy nor macular retinoschisis did differ between the DSM group and the non-DSM group ($P > 0.05$, respectively). However, the rate of patchy chorioretinal atrophy was significantly higher in the DSM group ($P < 0.001$).

Relationship Between Posterior Staphyloma and Dome-Shaped Macula

Among the eyes with DSM, 12 eyes had positive 3D MRI findings (Figure 1 and see **Figure, Supplemental Digital Content 1**, http://links.lww.com/IAE/B154, which showed 3D MRI eye imaging viewed at different angles of the other 9 eyes with irregular eye shapes combined with DSM). Nine eyes had horizontal oval-shaped dome, and a band-shaped inward convexity that extended horizontally from the optic disc through the fovea could be seen on 3D MRI. Three eyes had round dome, and 3D MRI showed a round inward convexity of the macular area. As to these inward convexities, five convexities were the border of multiple staphylomas (≥2 staphylomas) (Figure 1, A1–4), five were the boundary of one staphyloma (2 eyes had kidney-shaped staphyloma, Figure 1, B1–4), and two were just within a single staphyloma (the staphyloma of one eye was horizontally split into two parts by the band-shaped inward convexity, Figure 1, C1–4).

In the remaining six eyes that had a DSM but did not show any macular inward convexity on 3D MRI, the common feature was that OCT showed no obvious dome-shaped convexity of their vitreoretinal interface (Figure 2 and see **Figure, Supplemental Digital Content 2**, http://links.lww.com/IAE/B155, which showed the eye with a DSM and irregular eye shape but with no macular inward convexity on 3D MRI). Four eyes had obvious macular retinoschisis (Figure 2, A1–4). One eye had obvious macular pucker and a small foveal cystoid space (Figure 2, B1–4). The remaining eye had no other visible macular abnormalities on OCT except for a DSM.

Discussion

The DSM was first described by Gaucher et al[1] in 2008 as an inward bulge of the macula within a myopic PS. They have suggested that the decrease of visual acuity in patients with high myopia may be related to DSM.[1] These findings have attracted interest of many researchers. And most of the subsequent studies about DSM were based on OCT observations and data measurements.[3–6] However, the exact causes of DSM are still not well understood, and the relationship between

Table 1. Characteristics of the 18 Eyes (14 Patients) That Exhibited a DSM

Patient Number	Age (years)	Gender	Eye	Axial Length (mm)	Spherical Equivalent (D)	VA (Snellen)	Patchy Chorioretinal Atrophy	Choroidal Neovascularization Related Macular Atrophy	Type of DSM	Macular Retinoschisis	Retinal Detachment	Macular Hole	Macular Depression on 3D MRI
1	55	Male	Right	33.12	−21.5	CF	Present	Present	R	No	No	No	Yes
2	63	Male	Left	32.70	−16	20/125	Present	Absent	H	No	Yes	Yes	Yes
3	52	Female	Left	28.80	−26	20/400	Present	Absent	H	Yes	No	No	Yes
4	26	Female	Left	31.68	−20.5	20/63	Absent	Absent	H	No	No	No	No
5	77	Female	Right	30.02	−18	20/40	Present	Absent	R	Yes	No	No	Yes
			Left	27.53	−16	20/400	Present	Present	H	Yes	No	No	No
6	43	Female	Right	31.19	−23.75	20/125	Present	Absent	H	No	No	No	Yes
7	54	Female	Right	32.21	−19	20/100	Present	Absent	H	No	No	No	Yes
			Left	32.97	−20	20/63	Present	Absent	H	No	No	No	Yes
8	66	Female	Right	29.98	−13.75	20/63	Absent	Absent	H	Yes	No	No	No
			Left	29.65	−12.88	20/32	Absent	Absent	R	Yes	No	No	No
9	55	Female	Right	29.58	−10.75	20/400	Present	Present	H	No	No	No	Yes
			Left	31.50	−16.75	20/200	Present	Absent	H	No	No	No	Yes
10	65	Female	Right	26.95	−7	20/200	Absent	Absent	H	No	No	No	No
11	50	Female	Left	30.94	−20	20/200	Present	Present	H	No	No	No	Yes
12	46	Female	Left	27.60	−15	20/32	Absent	Absent	H	No	No	No	No
13	44	Female	Left	29.01	−20	CF	Absent	Absent	R	No	No	Yes	Yes
14	73	Female	Right	30.52	−17.25	20/100	Present	Absent	H	No	No	No	Yes

3D MRI, 3-dimensional magnetic resonance imaging; CF, counting finger; D, diopters; H, horizontal oval-shaped DSM; R, round DSM; VA, visual acuity.

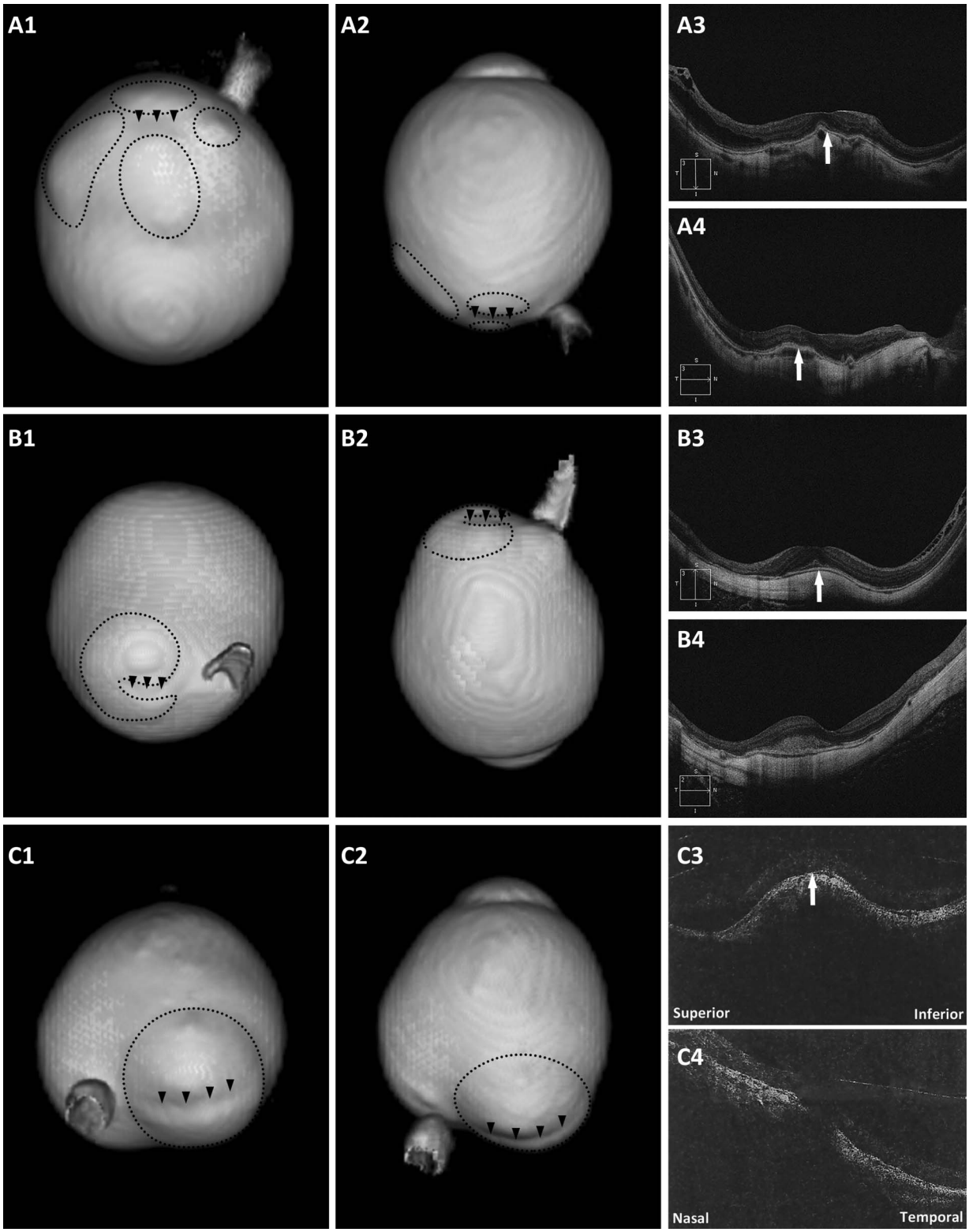

Fig. 1. Eyes with a DSM on OCT and a macular inward convexity on 3D MRI. **A1** and **A2.** Posterior view and side view of 3D MRI of the eye. One macular inward convexity (arrowheads) and four distinct staphylomas (circles) around are observed; (**A3** and **A4**) both vertical and horizontal scans show a convex macula (arrows). **B1** and **B2.** Posterior view and side view of 3D MRI of the eye. A band-shaped inward convexity (arrowheads) and a kidney-shaped staphyloma (circle) nearby are observed; (**B3**) vertical scan shows a clearly convex macula (arrow); (**B4**) horizontal scan shows a flat macula. **C1** and **C2.** Posterior view and side view of 3D MRI of the eye. The staphyloma (circle) was horizontally split into two parts by the band-shaped inward convexity (arrowheads); (**C3**) vertical scan shows a clearly convex macula (arrow); (**C4**) horizontal scan shows a slightly convex macula.

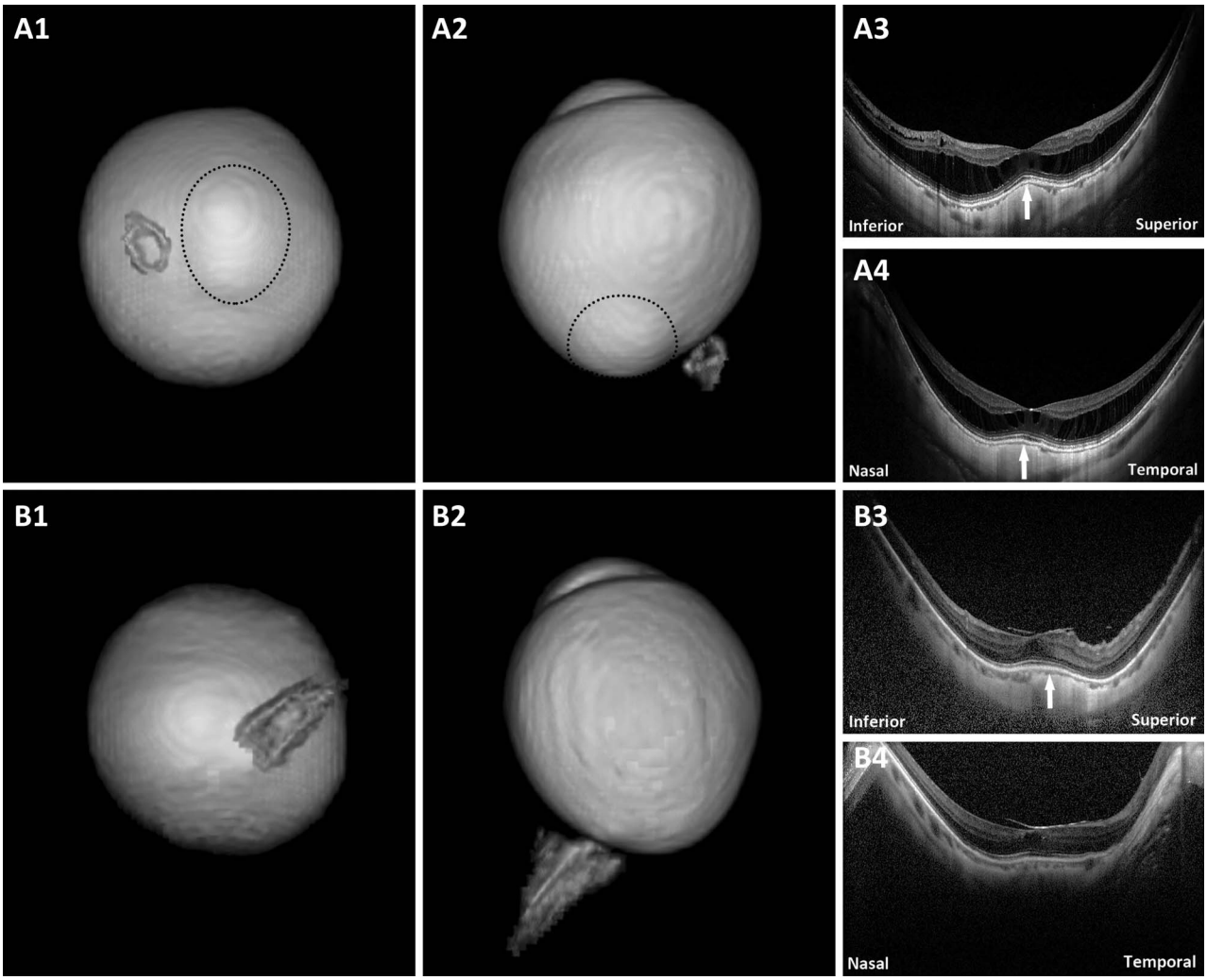

Fig. 2. Eyes with a DSM on OCT but with no macular inward convexity on 3D MRI. **A1** and **A2.** Posterior view and side view of 3D MRI of the eye. A staphyloma (circle) is observed; (**A3** and **A4**) both vertical and horizontal scans show a convex macula (arrows) and obvious macular retinoschisis. No obvious dome-shaped convexity of the vitreoretinal interface is observed. **B1** and **B2.** Posterior view and side view of 3D MRI of the eye. No protrusion or inward convexity is observed; (**B3**) vertical scan shows a clearly convex macula (arrow) and obvious macular pucker and a small foveal cystoid space. No obvious dome-shaped convexity of the vitreoretinal interface is observed; (**B4**) horizontal scan shows a flat macula and obvious macular pucker and a small foveal cystoid space.

PS and DSM remains unclear. Curtin[12] once classified PSs in eyes with pathologic myopia into 10 types based on wide-field stereoscopic ophthalmoscopy. Some studies have reported DSM could be seen in eyes with PS Type I, II, III, V, or IX.[9,13] In fact, there were also several studies about 3D OCT macular map reconstruction,[9,14,15] and three DSM patterns were observed, that is, vertical oval-shaped dome, horizontal oval-shaped dome, and round dome. But when it comes to the location relationship between DSM and PS, it seems that researchers preferred to express that DSM is located in a deep staphyloma, weakening the exact correspondence between them. We all know that a conventional OCT is unable to show the whole shape of the eyeball. This study combined 3D MRI with OCT so as to investigate the correlation between PS and DSM.

In 2014, Ohno-Matsui[16] used 3D MRI for analyzing the shape of eyes with and without a staphyloma. Six types of PSs were described according to their location and distribution. Nevertheless, only the contour of the outermost border of a PS was analyzed. Long-term observation of DSM has suggested that the sclera thickness of the central fovea is gradually thinning, but the thickness of the sclera is thicker than that of the circumferential concave and the macular bulge height is increasing gradually.[3,6] These hints suggest that we should pay attention to possible small staphylomas around DSM. Ohno-Matsui's classification of PS is not suitable for observing the relationship

between DSM and PS. In our study, we did not use a special classification of PS, as Ohno-Matsui[16] said that it is difficult to include many different kinds of scleral irregularities in the classification of staphylomas. The definition of PS here was "an outpouching of the wall of the eye that has a radius of curvature that is less than the surrounding curvature of the wall of the eye," as reported by Spaide.[11]

The DSM of high myopia accounted for 14.63% in this series, and the horizontal oval-shaped dome was the main type. These results were similar to those previous reports.[9,15,17,18] Two-thirds of the DSM had positive 3D-MRI findings. Nine eyes had horizontal oval-shaped dome, and a band-shaped inward convexity that extended horizontally from the optic disc through the fovea could be seen on 3D MRI. Three eyes had round dome, and 3D MRI showed a round inward convexity of the macular area. These findings correspond to the morphological observation of DSM on 3D OCT. As to these inward convexities, some were the border of multiple staphylomas, some were the boundary of one staphyloma, and the others were within a single staphyloma. It can be seen that there is an interesting correlation between DSM and PS. In 2011, Moriyama et al[7] used 3D MRI to analyze the eye shape of pathologic myopia. All of the eyes with three protrusions showed the DSM appearance on OCT scans. This is consistent with our observation that DSM could be the border of multiple staphylomas. These findings suggest that DSM is an abnormal shape of the entire posterior segment.

Of note, 6 eyes with DSM had no macular inward convexity on 3D MRI. When we reviewed the OCT of these eyes again, there was no obvious dome-shaped convexity of the vitreoretinal interface. Because T2-weighed images were used in 3D MRI, the outer surface of the eyeball imaging actually depicts the vitreoretinal interface.[16] This can explain why some DSM eyes had no macular inward convexity on 3D MRI.

Ohno-Matsui[16] pointed out that a DSM presented as a depression in 3D MRI viewed from the nasal side. Fifteen eyes of 27 eyes with myopic DSM had no apparent PS. There was no significant difference in the detection rate of DSM by 3D MRI in the eye with and without PS. She also pointed out that the resolution of MRI (1.5T) might limit the detection of shallow PS.[16] In this study, the layer thickness of the MRI (3.0T) was 0.6 $\sim$ 0.8 mm. Only one eye with DSM presented no PS or macular inward convexity on 3D MRI. Current studies have shown that DSM can be seen in people with emmetropia and hyperopia.[19,20] Therefore, whether DSM occurs before the formation of PS or whether DSM is a disease independent of PS remains to be determined.

The shortcomings of this study are as follows: First, the subjects included here were the patients with high myopia or its complications who were examined by 3D-MRI in our hospital, so there was a bias in selection. No eye was found with a vertical oval-shaped DSM. Second, 3D MRI cannot evaluate the scleral thickness change of PS because it reflects the vitreoretinal interface. Retinoschisis and circumscribed macular retinal detachment mentioned above will certainly affect the accuracy of judging a PS. Third, this study is cross-sectional, so additional longitudinal studies are needed to elucidate clearly the changes of PS in the formation of a DSM in myopic eyes. Finally, the detection rate of patchy chorioretinal atrophy in the DSM group was statistically higher than that in non-DSM group. One relevant study showed that the Bruch membrane rupture caused by patchy chorioretinal atrophy may be related to the formation of DSM.[21] The next research objective of our group is to explore the dynamic relationship of patchy chorioretinal atrophy, DSM, and PS.

In conclusion, 3D MRI is useful in analyzing the relative location relationship between PS and DSM. Highly myopic DSM mainly manifests as an inward convexity of the macular area on 3D-MRI viewed posteriorly. It can be the border of multiple PSs, the boundary of one staphyloma, or just within a single staphyloma. Its formation is related to the morphological change of the entire posterior segment.

Key words: dome-shaped macula, posterior staphyloma, OCT, 3D MRI.

References

1. Gaucher D, Erginay A, Lecleire-Collet A, et al. Dome-shaped macula in eyes with myopic posterior staphyloma. Am J Ophthalmol 2008;145:909–914.
2. Mehdizadeh M, Nowroozzadeh MH. Dome-shaped macula in eyes with myopic posterior staphyloma. Am J Ophthalmol 2008;146:478; author reply 478–479.
3. Soudier G, Gaudric A, Gualino V, et al. Long-term evolution of dome-shaped macula: increased macular bulge is associated with extended macular atrophy. Retina 2016;36:944–952.
4. Soudier G, Gaudric A, Gualino V, et al. Macular choroidal thickness in myopic eyes with and without a dome-shaped macula: a case-control study. Ophthalmologica 2016;236:148–153.
5. Byeon SH, Chu YK. Dome-shaped macula. Am J Ophthalmol 2011;151:1101–1102; author reply 1101–1102.
6. Ellabban AA, Tsujikawa A, Muraoka Y, et al. Dome-shaped macular configuration: longitudinal changes in the sclera and choroid by swept-source optical coherence tomography over two years. Am J Ophthalmol 2014;158:1062–1070.
7. Moriyama M, Ohno-Matsui K, Hayashi K, et al. Topographic analyses of shape of eyes with pathologic myopia by high-resolution three-dimensional magnetic resonance imaging. Ophthalmology 2011;118:1626–1637.
8. Tokoro T. Atlas of Posterior Fundus Changes in Pathologic Myopia: Springer; 1998:5–22.

9. Caillaux V, Gaucher D, Gualino V, et al. Morphologic characterization of dome-shaped macula in myopic eyes with serous macular detachment. Am J Ophthalmol 2013;156: 958–967 e951.
10. Wen B, Yang G, Cheng J, et al. Using high-resolution 3D magnetic resonance imaging to quantitatively analyze the shape of eyeballs with high myopia and provide assistance for posterior scleral reinforcement. Ophthalmologica 2017; 238:154–162.
11. Spaide RF, Ohno-Matsui K, Yannuzzi LA. Pathologic Myopia. New York, NY: Springer; 2014:167–177.
12. Curtin BJ. The posterior staphyloma of pathologic myopia. Trans Am Ophthalmol Soc 1977;75:67–86.
13. Coco RM, Sanabria MR, Alegría J. Pathology associated with optical coherence tomography macular bending due to either dome-shaped macula or inferior staphyloma in myopic patients. Ophthalmologica 2012;228:7–12.
14. Ellabban AA, Tsujikawa A, Matsumoto A, et al. Three-dimensional tomographic features of dome-shaped macula by swept-source optical coherence tomography. Am J Ophthalmol 2013; 155:320–328 e322.
15. Garcia-Ben A, Kamal-Salah R, Garcia-Basterra I, et al. Two- and three-dimensional topographic analysis of pathologically myopic eyes with dome-shaped macula and inferior staphyloma by spectral domain optical coherence tomography. Graefes Arch Clin Exp Ophthalmol 2017;255:903–912.
16. Ohno-Matsui K. Proposed classification of posterior staphylomas based on analyses of eye shape by three-dimensional magnetic resonance imaging and wide-field fundus imaging. Ophthalmology 2014;121:1798–1809.
17. Ohsugi H, Ikuno Y, Oshima K, et al. Morphologic characteristics of macular complications of a dome-shaped macula determined by swept-source optical coherence tomography. Am J Ophthalmol 2014;158:162–170.e161.
18. Liang IC, Shimada N, Tanaka Y, et al. Comparison of clinical features in highly myopic eyes with and without a dome-shaped macula. Ophthalmology 2015;122:1591–1600.
19. Errera MH, Michaelides M, Keane PA, et al. The extended clinical phenotype of dome-shaped macula. Graefes Arch Clin Exp Ophthalmol 2014;252:499–508.
20. Kedkovid N, Afshar AR, Damato BE, Stewart JM. Dome-shaped macula with thickened choroid in an emmetropic patient. Retin Cases Brief Rep 2015;9:307–310.
21. Fang Y, Jonas JB, Yokoi T, et al. Macular Bruch's membrane defect and dome-shaped macula in high myopia. PLoS One 2017;12:e0178998.